Circular flight kite tests: converting to standard results

J. C. Stevenson
Syft
Christchurch, New Zealand

K. V. Alexander
University of Canterbury
Christchurch, New Zealand

ABSTRACT

Kite testing by flying in a horizontal circle, was developed in order to address the inevitable accuracy problems inherent in pre-existing kite measurement techniques. However the raw results from this circular flight method are not directly comparable with traditional kite performance measurements. To enable direct comparisons to be made, modifying equations have been developed to convert the raw circular flight results into the traditional measurements of lift to drag ratio, and lift coefficient. This paper derives the modifying equations, and presents experimental results comparing traditional measurements with both the raw and modified circular flight results. The modifying equations are applied to an example set of results to assess the sensitivity of the test environment parameters. It is concluded that for many cases, the discrepancy between the raw circular flight test results and traditional measurement techniques is small enough to ignore. Alternatively, the modifying equations given in the paper may readily be encoded so that traditional results may be quickly obtained from this novel test method.

NOMENCLATURE

A	kite surface area (not projected area, see Ref. 1) (m^2)
CD_{linej}	drag coefficient on the jth line element. (Equation (8))
CL	lift coefficient based on the aerodynamic lift L (Equation (38))
CL_{linej}	lift coefficient on a jth line element. (Equation (7))
CL_T	total lift coefficient of the kite/line system in circular flight testing, based on the force at the flier (N) (Fig. (14) (Equation (4))
D	kite aerodynamic drag (N) (Figs 4 and 12) (Equation (31))
D_{cent}	summed centrifugal forces of all lines; component acting in the direction of the kite drag (N) (Equation (27))
D_l	aerodynamic and centrifugal forces of the line acting in the direction of the kite drag (N) (Fig. 4) (Equation (29))
D_{LA}	summed aerodynamic forces of all lines; the component in the direction of the kite drag (N) (Equation (25))
D_{LAj}	aerodynamic forces of the jth line element in the drag direction, at a point P on the line (N) (Equation (10))
D_T	total drag force of the kite and line system as measured in circular flight (N) (Fig. 4) (Equation (30))
F_{cj}	centifugal force of the jth line element (N) (Equation (11))
g	gravitational acceleration (ms^{-2})
j	arbitrary element number for the elements the kite line is divided up into for numerical analysis.
k	distance to line inflexion point from kite as a proportion of S; proportion of the line weight m_l carried by the kite (Fig. 12) (Equation (36))
L	kite aerodynamic lift (N) (Fig. 37) (Equation (39))
L/D	lift to drag ratio of the aerodynamic surface (ignoring weight effects and effects of the kite line and bridle)
L_c	kite lift component in the horizontal plane, with line effects removed (N) (Fig. 4) (Equation (32))

Paper No. 3050. Manuscript received 22 December 2005, accepted 16 May 2006.

https://doi.org/10.1017/S0001924000001469 Published online by Cambridge University Press

L_{cent} summed centrifugal force of all lines; component in the direction of the kite aerodynamic lift (N) (Equation (26))
L_h kite lift component in the horizontal plane with the centrifugal force and the line effects removed (N) (Figs 4 and 12) (Equation (34))
L_l aerodynamic and centrifugal forces of the line acting parallel to the kite lift direction. (N) (Note that L_l usually acts towards the flyer, making it negative in calculations) (Fig. 4) (Equation (28))
L_{LA} summed aerodynamic forces of all lines; the component in the kite (horizontal) lift direction (N) (Equation (24))
L_{LAj} aerodynamic forces of the *j*th line element in the (horizontal) lift direction, at a point *P* (N) (Equation (9))
L_T total horizontal component of the lift force of the kite/line system (N) (Fig. 4) (Equation (3))
L_T/D_T lift to drag ratio of the kite/line system as measured at the flier in circular flight in the horizontal plane. (Equation (1))
LTD_k lift to drag ratio of the kite, as measured at the kite when flown in the normal elevated position, with the kite weight included; effects of the line are not included. (Equation (39))
M mass of kite (kg) (Equation (39))
m_l total mass of all lines (kg) (Equation (36))
m_{line} line mass (of a single line) per unit length (kg/m) (Equation (26))
n number of lines (Equations (24-26))
N_{cj} centrifugal force coefficient for a *j*th line element (Equation (19))
N_{DA} line aerodynamic force coefficient in kite (horizontal) drag direction (Fig. 8) (Equation (18))
N_{DAj} drag force for a *j*th line element in the kites drag direction (N) (Equation (16))
N_{DC} lines total centrifugal force coefficient in kite (horizontal) drag direction (Fig. 10) (Equation (24))
N_{DCj} centrifugal for a *j*th line element in the kites drag direction (N) (Equation (23))
N_{LA} lines total aerodynamic force coefficient in kite (horizontal) lift direction (Fig. 7) (Equation (17))
N_{LAj} lift force for a *j*th line element in the kite's drag direction (N) (Equation (15))
N_{LC} lines total centrifugal force coefficient in kite (horizontal) lift direction (Fig. 9) (Equation (22))
N_{LCj} centrifugal for a *j*th line element in the kite's lift direction (N) (Equation (20))
R radius of the kite's circular flying path (*m*) (Figs 1 and 2) (Equation (6))
R_j radius to the general point P on the *j*th line element (m) (Figs 5 and 6) (Equation (12))
r radius of the flyer's walking circle when flying the kite in a circle (m) (Figs 1 and 2)
S line length (m) (Figs 1 and 2)
S_j distance from the flyer to the point *P* on the *j*th line element (m) (Equation (12))
T total aerodynamic force exerted by kite (with mass, centrifugal force and line effects removed) (N) (Figs 11 and 12) (Equation (36))
T_c horizontal component of the resultant kite force, with line effects removed (N) (Figs 3 and 4) (Equation (33))
T_h horizontal component of the resultant kite force, with line effects and centrifugal force removed (N) (Figs 11 and 12) (Equation (35))
T_k resultant line force at the top of the line (at the kite) for a real kite with mass flying in the normal elevated position. (N) (Equation (40))
T_T total force exerted by the kite/line system at the flyer, as measured in circular flight (N) (Fig. 4)
V_j velocity at the 'jth' line segment (ms^{-1}) (Figs 3, 5 and 6) (Equation (11))

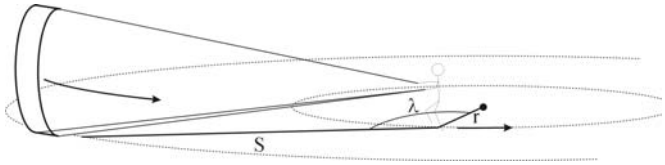


Figure 1. Flying a kite in a circle.

V_k velocity of the kite (ms^{-1}) (Fig. 2) (Equation (5))
V_w walking speed of the flyer (ms^{-1}) (Fig. 2)
z number of elements the kite line is divided up into, for numerical analysis (Equations (17), (18), (22) and (23))
β performance angle of the kite during tests: $L_T/D_T = 1/\mathrm{Tan}(\beta)$ (deg) (Fig. 4) (Equation (1) and (2))
ϕ line diameter (m)
λ angle between the kite line *S*, and the walking radius *r* (Fig. 2)
ρ density of air (kg/m^3)
ω_φ angle between the line and the apparent wind at the *j*th line segment (deg) (Figs 5 and 6) (Equations (7), (8) and (13))

1.0 INTRODUCTION

Previous papers by the authors[1,2] have presented the fundamentals of measuring kite performance using circular flight tests. These have demonstrated that the method can provide more accurate results than traditional testing methods, such as stationary flight in natural wind or car-based tests in still air[3]. The essence of the method involves flying the kite in circles parallel to the ground as shown in Fig. 1. By doing this the performance of the kite (lift to drag ratio) can be approximately determined from the line length *S*, the radius of the 'walking circle' *r*, and the angle λ between this radius and the line(s). The lift coefficient can be found once the walking speed V_w and line load T_T are also measured. Since the geometry of the test setup can be tuned for each test kite, errors related to line angle measurements can be kept to a minimum.

Unfortunately, as the kite flies in a circle there are extra forces present that make the raw performance results different to those obtained using more traditional measurements such as wind tunnel testing or car rig testing[2]. Despite this, the raw results still reflect the underlying performance of the kite and they can be used comparatively for performance improvement programs.

It is useful however, to have the traditional results of *L*/*D* and *CL* for direct comparison with data from other sources. The purpose of this paper therefore, is to develop the equations that map the raw results from circular testing on to the traditional kite performance measurements. It compares the results to those derived from other tests in Figs 13 and 14. It then goes on to give an example set of calculations and a sensitivity analysis to illustrate the scale of the circular flight effects in the raw measured results.

2.0 CIRCULAR FLIGHT PERFORMANCE MEASUREMENTS

The full derivations of the equations for circular flight testing were shown by Stevenson, Alexander and Lynn[2]. The pertinent results are repeated here in Equations (1) to (6). Note that for raw circular flight test results the symbols are given the subscript *T* (for test). The raw lift to drag ratio from circular testing can be seen from Fig. 2 to be based on the lengths *S* and *r*, and the angle λ measured at the flier. It is defined as:

https://doi.org/10.1017/S0001924000001469 Published online by Cambridge University Press

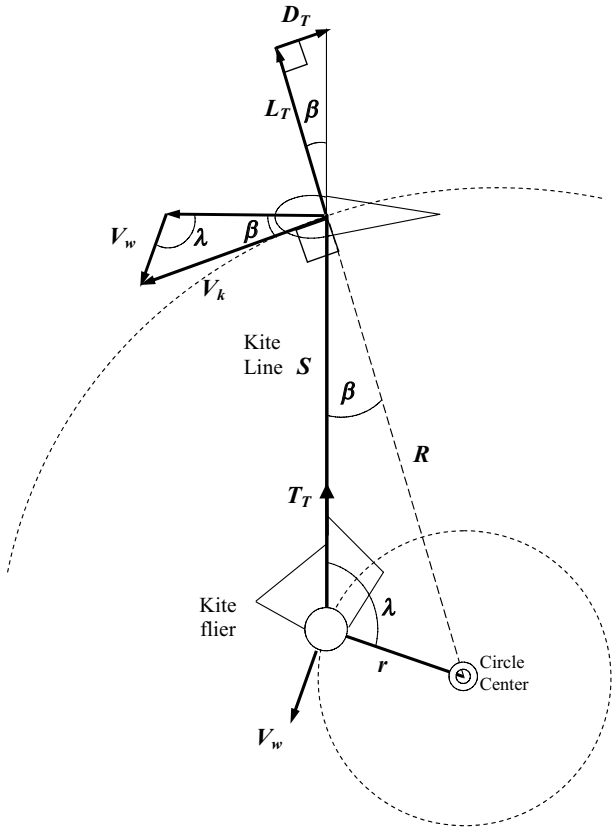


Figure 2. Plan view of a circular flight test.

$$\frac{L_T}{D_T} = \frac{1}{\mathrm{Tan}(\beta)} \quad \ldots (1)$$

where L_T, D_T and β can be seen in Fig. 2 and

$$\beta = \mathrm{Sin}^{-1}\frac{r.\mathrm{Sin}(\lambda)}{\sqrt{r^2 + S^2 - 2rS\mathrm{Cos}(\lambda)}} \quad \ldots (2)$$

derived from Fig. 2 in Equation (12) of Ref. 2.

By measuring the tension in the kite lines (T_T) the 'lift' force (in this case measured in the horizontal plane) can be determined using:

$$L_T = T_T\mathrm{Cos}(\beta) \quad \ldots (3)$$

This force can then be converted into a lift coefficient using the usual definition.

$$CL_T = \frac{L_T}{\frac{1}{2}\rho A V_k^2} \quad \ldots (4)$$

where

$$V_k = V_w\frac{R}{r} \quad \ldots (5)$$

which is apparent from Fig. 2. R can be found from the same figure by:

$$R = \sqrt{r^2 + S^2 - 2rS\mathrm{Cos}(\lambda)} \quad \ldots (6)$$

3.0 REMOVING THE CIRCULAR FLIGHT EFFECTS

The lift to drag ratio of Equation (1) and the lift coefficient of Equation (4) are not the same as the aerodynamic measures of L/D and CL for the following reasons:

1. Because the kite is flying in a horizontal circle it is subjected to centrifugal forces.
2. Because of the kite orientation during flight, the weight of the kite no longer acts in the same plane as the lift and drag forces.
3. The forces on the kite lines are considerably different from the forces on the lines when a kite is flying in its normal orientation. In circular flight the lift and drag forces of the lines themselves vary along the line length as the apparent wind increases with radius. The circular flight path also adds centrifugal forces to the contribution from the lines, (because of the line mass).

Figure 3 shows how these line forces affect the system while Fig. 4 is a plan view of the vector diagrams used to derive the equations.

Converting the lift to drag ratio found in the test L_T/D_T , into the traditional form L/D is done using broadly the following process:

- Take a set of measurements to obtain the line load T_T and, from the geometry, the performance angle β.
- From the total measured load T_T, remove the aerodynamic and centrifugal forces resulting from the lines to arrive at T_c, the load applied by the kite to the line.
- From T_c remove those loads arising from centrifugal force of the kite itself, to arrive at T_h, the component of kite aerodynamic load in the horizontal plane.

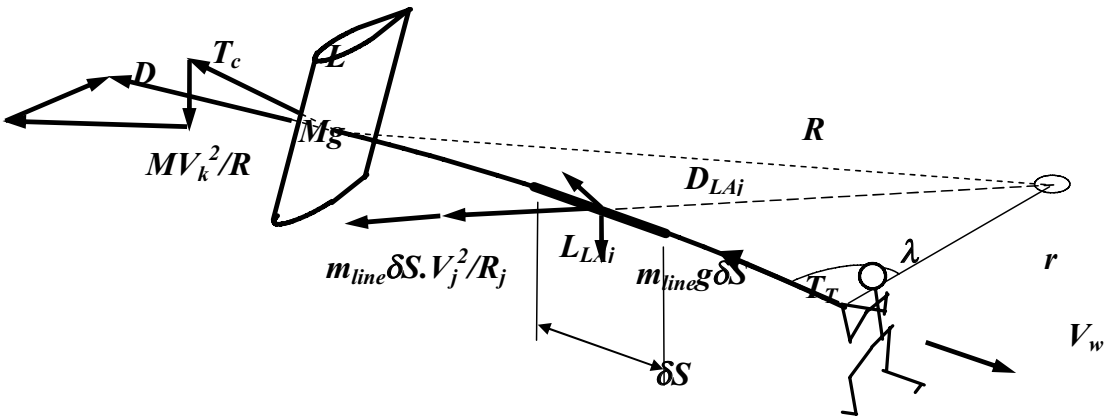


Figure 3. Forces and geometry of the system.

https://doi.org/10.1017/S0001924000001469 Published online by Cambridge University Press

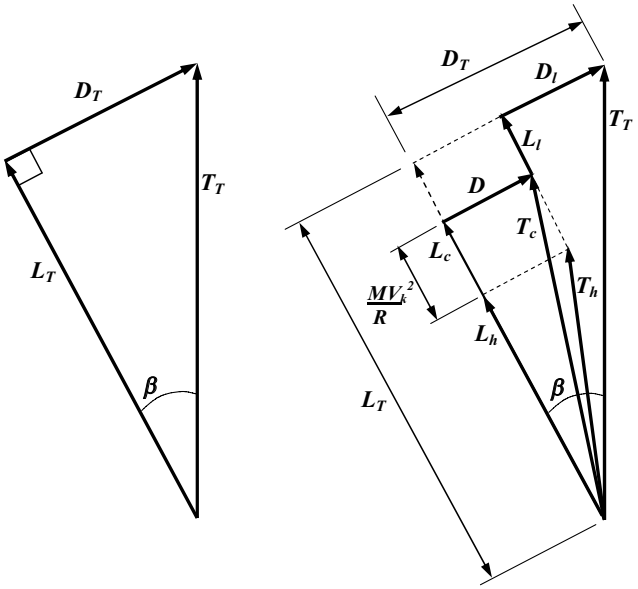


Figure 4. Plan view of force vectors.

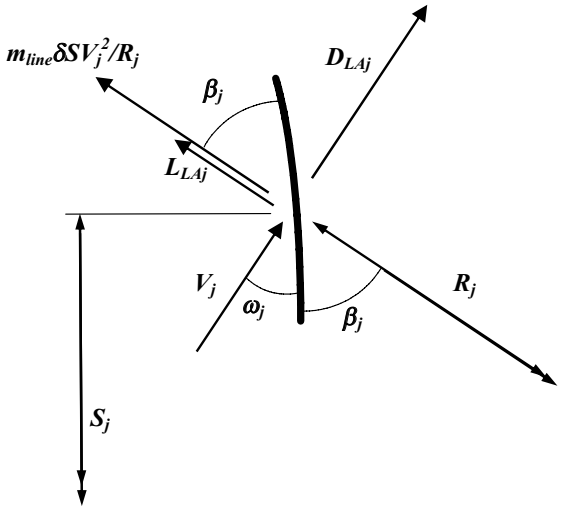


Figure 5. Forces on the *j*th line segment of length δS.

- From T_h make an adjustment for the kite and line weight forces to arrive at T, the kite resultant aerodynamic force.
- From this the net aerodynamic L/D and CL can be found.

The paper systematically derives the necessary equations so that each step builds on the one before. Throughout this analysis De Lambert's theorem has been used to account for the centrifugal forces rather than Newton's method. This allows the problem to be considered as a statics problem.

3.1 Removing the line loads

The strategy to remove the effect of the kite lines from circular test results is to determine the horizontal line loads from known methods, then project them on to the lift and drag force directions of the kite wing. The line loads in the kite lift and drag directions are designated L and D_l as in Fig. 4.

The method to determine the line forces rests on being able to divide the line into a number (z) of small segments, each with a length ds. A comprehensive analysis of a straight section of line has been provided by Goela[4], and applied to the kite testing situation by Stevenson[1]. In the analysis here it has been assumed that the line is more or less straight, which is not unrealistic for the circular test situation as discussed in Ref. 1. However, the line environment in circular flight testing is more complicated than with stationary kites as will be demonstrated.

Figures 3 and 5 show the line forces acting on the *j*th segment of a single line of length ds. The primary forces acting on the line are the lift and drag forces which act perpendicular and parallel the wind direction respectively. The lift and drag coefficients acting on a segment of line have been given by Hoerner[5] as:

$$CL_{linej} = 1 \cdot 1 \mathrm{Sin}^2(\omega_j)\mathrm{Cos}(\omega_j) \quad \ldots (7)$$

and

$$CD_{linej} = 1 \cdot 1 \mathrm{Sin}^3(\omega_j) + 0 \cdot 02 \quad \ldots (8)$$

where the line coefficients are defined as:

$$CL_{linej} = \frac{L_{LAj}}{1/2 \rho \phi V_j^2 ds} \quad \ldots (9)$$

$$CD_{linej} = \frac{D_{LAj}}{1/2 \rho \phi V_j^2 ds} \quad \ldots (10)$$

These expressions represent the forces in the direction perpendicular to the local flow (L_{LAj}) and parallel to the flow (D_{LAj}).

Figures 3 and 5 also show the centrifugal forces on the *j*th segment of a single line. Since the element of line δs is moving in a circle it is also subject to a centrifugal force which acts along the circle radius. The centrifugal force on this element is equal to:

$$F_{cj} = \frac{m_{line} \delta S . V_j^2}{R_j} \quad \ldots (11)$$

It is not straightforward to simply sum the aerodynamic and centrifugal forces over the length of the line. Since the kite is flying in a circle, the aerodynamic forces increase along the length of the line as apparent air speed increases with line radius. The centrifugal force also varies as the radius increases. The directions of both sets of forces are not in the direction of the line but are related to the line angle measurement λ. These effects make an analytical solution over the whole line for Equations (7), (8) and (11), quite unmanageable. So instead of an analytical solution, the process has been to sum the individual coefficients of each line segment to arrive at combined coefficients for the full line length. These combined coefficients are then plotted so they can be used in subsequent calculations without the need to derive them each time.

3.1.1 Geometry of line segments

First, the unknown, ω_j in Equations (7) and (8) needs to be found. From Figs 3, 5 and particularly Fig. 6 it can be shown that the radius R_j to any point P, on the line is:

$$R_j = \sqrt{r^2 + S_j^2 - 2r.S_j \mathrm{Cos}(\lambda)} \quad \ldots (12)$$

and using R_j, the angle ω_j between the flow and the line at P is:

$$\omega_j = 90 - \mathrm{Sin}^{-1}\left(\frac{r}{R_j}.\mathrm{Sin}(\lambda)\right) \quad \ldots (13)$$

The velocity V_j at P is found from the measured walking speed V_w

https://doi.org/10.1017/S0001924000001469 Published online by Cambridge University Press

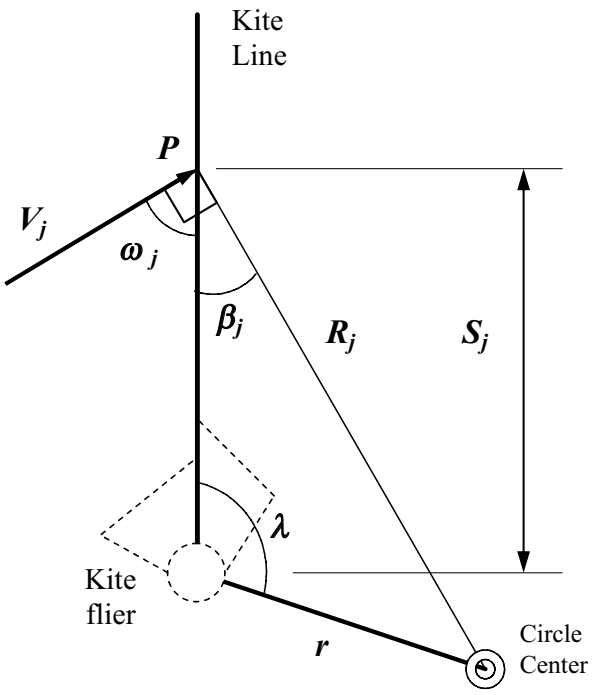


Figure 6. Geometry and conditions at a general point *P* on the kite line.

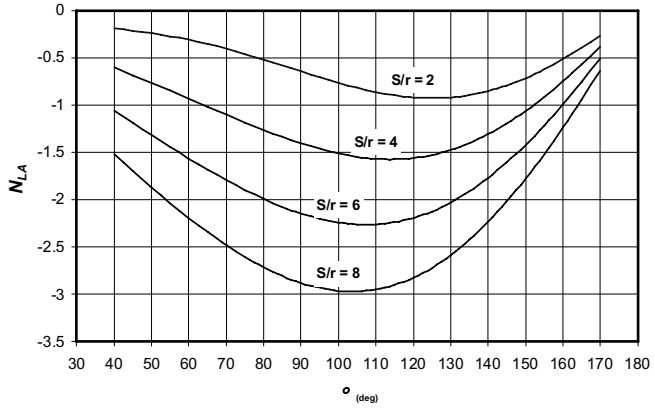


Figure 7. Line aerodynamic force coefficient in kite lift direction.

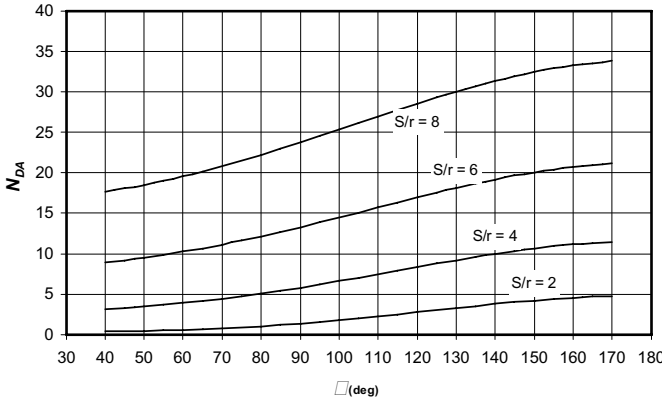


Figure 8. Line aerodynamic force coefficient in kite drag direction.

and R_j:

$$V_j = V_w \frac{R_j}{r} \quad \ldots (14)$$

3.1.2 Coefficients N_{LA} and N_{DA} for the aerodynamic loads of a single line

Now ω_j may be substituted back into Equations (7) and (8) to find the coefficients CL_{linej} and CD_{linej} at the *j*th small section of line around the point *P*.

Since the lift and drag force directions change with the angle ω from the flyer to the kite, it is useful to project them on to a common direction. The directions of choice are the directions of the kite lift and drag forces. Further, as the apparent air speed varies along the line, these coefficients need to be normalised as well. So the coefficients for the *j*th line segment, projected and normalised are therefore:

$$N_{LAj} = \left(CD_{linej}\mathrm{Cos}(\beta+\omega_j) - CL_{linej}\mathrm{Sin}(\beta+\omega_j)\right)\frac{V_j^2}{V_w^2} \quad \ldots (15)$$

$$N_{DAj} = \left(CD_{linej}\mathrm{Sin}(\beta+\omega_j) + CL_{linej}\mathrm{Cos}(\beta+\omega_j)\right)\frac{V_j^2}{V_w^2} \quad \ldots (16)$$

These coefficients are now found for every section of line from $j = 1$ to $j = z$. Then the results are summed over the length of the line to give coefficients that represent the whole line length:

$$N_{LA} = \frac{1}{z}\sum_{j=1}^{z} N_{LAj} \quad \ldots (17)$$

$$N_{DA} = \frac{1}{z}\sum_{j=1}^{z} N_{DAj} \quad \ldots (18)$$

These coefficients have been plotted for useful ranges of *S*/*r* and λ in Figs 7 and 8.

3.1.3 Coefficients N_{LC} and N_{DC} for the centrifugal loads of a single line

Now the task is to find coefficients for the centrifugal forces along the whole length of line. For the *j*th small segment the centrifugal force F_{cj} has been given above in Equation 11. A suitable coefficient, normalised by the walking speed and the radius may be given by:

$$N_{cj} = \frac{S}{R_j}\frac{V_j^2}{V_w^2} \quad \ldots (19)$$

The centrifugal force represented by this coefficient acts radially outwards from the circle centre. In the same way as done for the aerodynamic coefficients, it is projected on to the kite lift and drag directions using:

$$N_{LCj} = N_{cj}\mathrm{Sin}(\beta+\omega_j) \quad \ldots (20)$$

$$N_{DCj} = -N_{cj}\mathrm{Cos}(\beta+\omega_j) \quad \ldots (21)$$

As before, the coefficients are evaluated for every section of the line from $j = 1$ to $j = z$. These are then summed over the length of the line to give the coefficients N_{LC} and N_{DC} for the centrifugal force for the whole line length projected on to the kite lift and drag directions:

https://doi.org/10.1017/S0001924000001469 Published online by Cambridge University Press

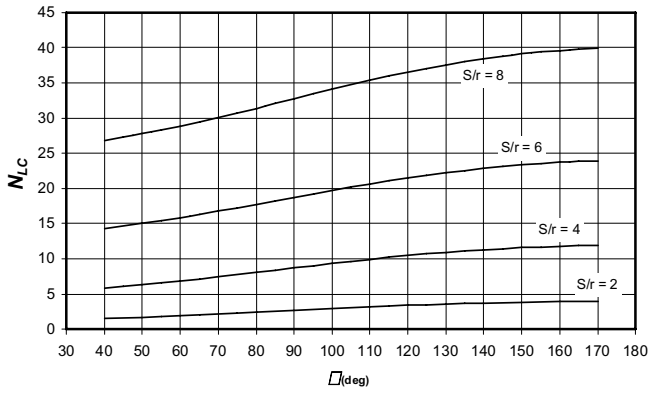


Figure 9. Line centrifugal force coefficient in kite lift direction.

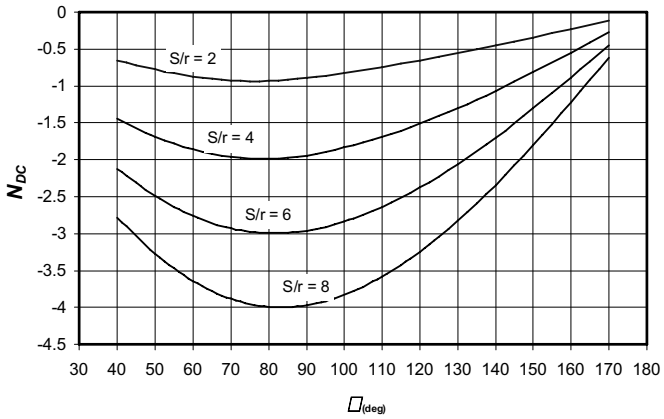


Figure 10. Line centrifugal force coefficient in kite drag direction.

$$N_{LC} = \frac{1}{z}\sum_{j=1}^{z} N_{LCj} \quad \ldots (22)$$

$$N_{DC} = \frac{1}{z}\sum_{j=1}^{z} N_{DCj} \quad \ldots (23)$$

These coefficients have been plotted for the useful ranges of S/r and λ in Figs 9 and 10.

3.1.4 The line loads L_l and D_l

Now that the coefficients are established, the line loads in the kite lift and drag directions can readily be found. Using the geometry of the test setup, the number of lines used n, their diameter ϕ, the mass per unit length m_{line}, and the appropriate coefficients from Figs 7 to 10, the aerodynamic forces L_{LA} and D_{LA} can be found for any instance from:

$$L_{LA} = \frac{1}{2} S\phi\rho V_w^{\,2} n N_{LA} \quad \ldots (24)$$

$$D_{LA} = \frac{1}{2} S\phi\rho V_w^{\,2} n N_{DA} \quad \ldots (25)$$

And the centrifugal forces L_{cent} and D_{cent} can be found from:

$$L_{cent} = m_{line} V_w^{\,2} n N_{LC} \quad \ldots (26)$$

$$D_{cent} = m_{line} V_w^{\,2} n N_{DC} \quad \ldots (27)$$

Using the results from Equations 24 to 27, the line forces in the kite lift and drag directions L_l and D_l, can be found from:

$$L_l = L_{LA} + L_{cent} \quad \ldots (28)$$

$$D_l = D_{LA} + D_{cent} \quad \ldots (29)$$

It should be noted that if the geometry of the test remains constant (S/r and λ constant) then L_l and D_l will vary with the square of the speed, so the ratio L_l/D_l will remain constant. As a result, in repeated tests of the same geometry, these line loads need only be calculated once, and then scaled with the square of the speed.

3.2 Load equations with line loads removed

It is possible to write a number of equations directly from the vector diagram of (horizontal) forces in Fig. 4. Beginning with the measured line tension T_T, and the angle β (found from the measured λ in Equation 2), it can be seen in Fig. 4 that:

$$D_T = T_T \mathrm{Sin}(\beta) \quad \ldots (30)$$

$$L_T = T_T \mathrm{Cos}(\beta) \quad \text{repeated from (3)}$$

Now equations can be written for the kite lift, drag and resultant forces with the line loads removed. (The forces T_c and L_c are given the subscripts 'c' to indicate that the effect of the kite centrifugal force is still present. The drag contains no centrifugal component so has no such subscript). Again from Fig. 4:

$$D = D_T - D_l \quad \ldots (31)$$

$$L_c = L_T - L_l \quad \ldots (32)$$

$$T_c = \sqrt{L_T^{\,2} + D^2} \quad \ldots (33)$$

3.3 Removing the centrifugal force of the kite itself

Because the kite has a certain mass there is a centrifugal force applied by the kite to the line as the kite flies in its circular path. This force needs to be separated out from the aerodynamic forces under test. In Fig. 4 the centrifugal force MV_k^2/R is shown acting in the same direction as the lift, radially outwards from the circle centre. The drag D is unaffected by the centrifugal force components. The equations for the kite loads in the horizontal plane (subscript 'h'), with centrifugal forces removed, can be written directly from the figure and the previous section:

$$L_h = L_c - \frac{MV_k^{\,2}}{R} \quad \ldots (34)$$

$$T_h = \sqrt{L_h^{\,2} + D^2} \quad \ldots (35)$$

3.4 Removing the effect of the kite weight

Referring now to Fig. 11 it can be seen that the resultant aerodynamic force T, generated by the kite must have a vertical component in order for the kite and line not to fall to the ground. Knowing the kite mass M, and the proportion of the line mass it carries, $k \cdot m_l$, the kite resultant aerodynamic force T can be derived from Fig. 12. (The variable k, the proportion of the line mass that the kite lifts is also the distance to the inflexion point of the line from the kite, as a proportion of the line length. If the line is close to horizontal as in most test cases, k can be approximated as 0·5). So from Fig. 12:

https://doi.org/10.1017/S0001924000001469 Published online by Cambridge University Press

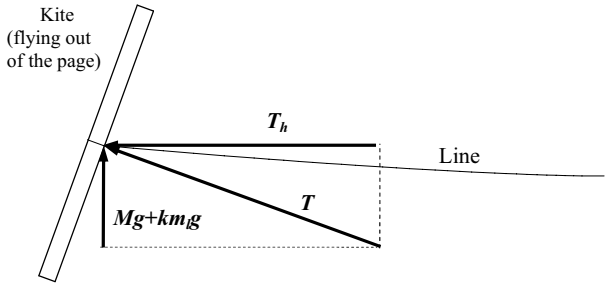


Figure 11. Kite loads in the vertical plane.

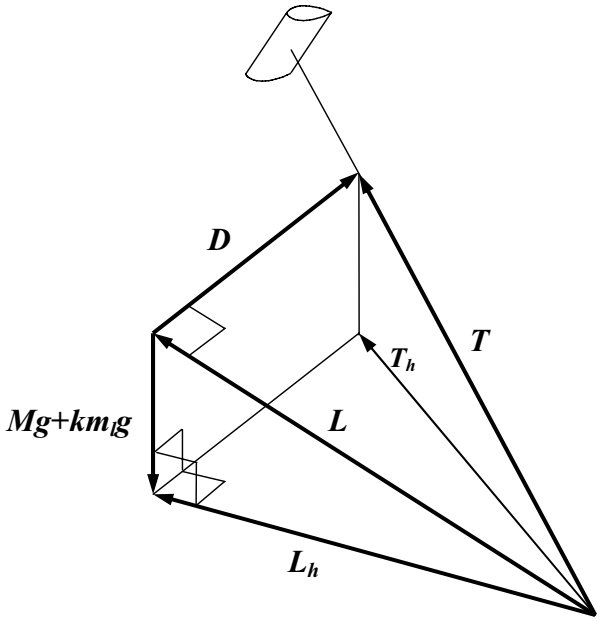


Figure 12. Vector diagram showing the net aerodynamic loads *T*, *L* and *D*.

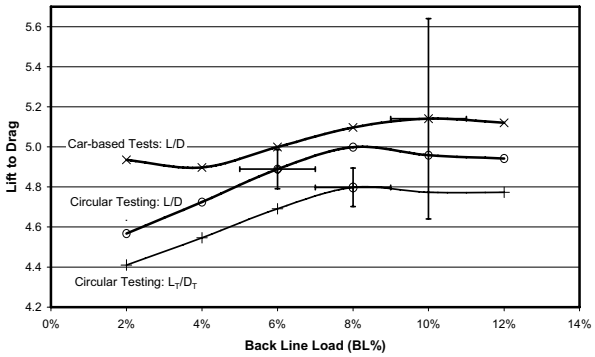


Figure 13. Lift to drag results, comparing the car based rig *L*/*D*, circular flight testing corrected results *L*/*D*, and circular flight testing raw results L_T/D_T, for a 3.2 C-Quad kite.

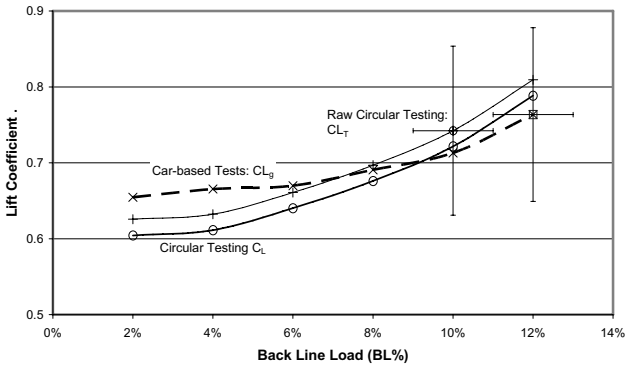


Figure 14. Lift coefficient results, comparing the car-based rig *CLg*, circular flight testing corrected results C_L, and circular flight testing raw results CL_T, for a 3.2 C-Quad kite.

$$T = \sqrt{T_h^{\,2} + (Mg + k.m_l.g)^2} \qquad \ldots (36)$$

And finally the net aerodynamic lift of the kite surface is:

$$L = \sqrt{T^2 - D^2} \qquad \ldots (37)$$

4.0 PERFORMANCE EQUATIONS

The lift to drag ratio from purely aerodynamic forces, *L*/*D* can be written directly from Equations (31) and (37). The lift coefficient *CL* from purely aerodynamic forces alone, may be written using the aerodynamic lift *L*, from Equation (37):

$$CL = \frac{L}{0 \cdot 5\rho V_k^{\,2} A} \qquad \ldots (38)$$

From a purist point of view this is all that is necessary, but practical kite usage dictates that the results are more useful with the kite weight taken into account for the case of elevated vertical flight. As described in Ref. 6, the lift to drag ratio with kite weight taken into account LTD_k, is given by:

$$LTD_k = \frac{L - Mg}{D} \qquad \ldots (39)$$

The resultant line force at the top of the line (at the kite) for a real kite with mass is given by:

$$T_k = \sqrt{(L - Mg)^2 + D^2} \qquad \ldots (40)$$

5.0 SAMPLE TEST RESULTS

The plots in Figs 13 and 14 are test results from the reference kite used in Ref. 1, which was a four-line traction kite. The results are plotted against the percent of total load taken by the back (aft) pair of lines. This variable is used as it is the primary way a flier can influence the performance of a kite. (Increasing the proportion of load on the back lines increases the angle-of-attack.). These figures show the lift-to-drag ratio and the lift coefficient, and compare:

- Results from the car rig
- Raw results from circular flight testing described in Ref. 2
- Modified results from circular flight testing, using the methods of this paper.

https://doi.org/10.1017/S0001924000001469 Published online by Cambridge University Press

Table 1
Sample set of measurements

Walking radius	r	7·5	m
Kite line length	S	30	m
Walking speed	V_w	2·5	ms^{-1}
Number of kite lines	n	4	
Density of air	ρ	1·23	kg/m^3
Kite line diameter	ϕ	0·002	m
Kite area	A	3	m^2
Line mass per unit length	m_{line}	0·00346	kg/m
Kite mass	M	0.5	kg
Test Results			
Angle between r and S (Fig. 2)	λ	105	deg
Total force exerted by the kite/line system at the flier	T_T	300	N

Table 2
Calculated results (no adjustment for circular flight yet)

	Equation			
Kite performance angle	2	β	12·78	deg
Kite apparent wind velocity	5	V_k	10·9	ms^{-1}
Kite radius from circle centre	6	R	32·75	m
Mass of all line ($m_{line} \times S \times n$)		m_l	0·415	kg
Lift from unmodified circular test results	3	L_T	293	N
Drag from unmodified circular test results	30	D_T	66·4	N
Lift to drag ratio from unmodified test results	1	L_T/D_T	4·41	
Lift coefficient in unmodified circular test results	4	C_{LT}	0·733	

Table 3
Line loads in kite (horizontal) lift and drag directions

Coefficient for line aero force in lift direction	Fig. 7	N_{LA}	–1·55	
All lines aerodynamic force in kite lift direction	Equation (24)	L_{LA}	–1·43	N
Coefficient for line aero force in drag direction	Fig. 8	N_{DA}	7·04	
All lines aerodynamic force in kite drag direction	Equation (25)	D_{LA}	6·50	N
Coefficient for line centrifugal force in lift direction	Fig. 9	N_{LC}	9·67	
All lines centrifugal force in kite lift direction	Equation (26)	L_{cent}	0·835	N
Coefficient for line centrifugal force in drag direction	Fig. 10	N_{DC}	–1·77	
All lines centrifugal force in kite drag direction	Equation (27)	D_{cent}	–0·153	N
Total line load in the kite lift direction	Equation (28)	L_l	–0·593	N
Total line load in the kite drag direction	Equation (29)	D_l	6·35	N

Table 4
Kite horizontal loads with line loads removed

	Equation			
Lift (horizontal, including centrifugal force)	32	L_c	293·2	N
Drag (net aerodynamic drag)	31	D	60·01	N
Lift to drag ratio (horizontal, including centrifugal force)		L_c/D	4·89	

Table 5
Kite horizontal loads with both line loads and centrifugal loads removed

	Equation			
Lift (horizontal)	34	L_h	291·3	N
Drag (net aerodynamic drag)	31	D	60·01	N
Lift to drag ratio (horizontal)		L_h/D	4·855	

Table 6
Kite net aerodynamic loads: All circular flight, weight and line loads removed

	Equation			
Lift (net aerodynamic lift)	37	L	291·4	N
Drag (net aerodynamic drag)	31	D	60·01	N
Lift-to-drag ratio (net aerodynamic)		L/D	4·856	
Lift coefficient	38	CL	0·736	
Resultant aerodynamic force	36	T	297·54	N

Table 7
Test results converted for a kite of the same mass flown vertically(no line loads)

	Equation			
Lift (kite mass included): L-Mg			286·5	N
Drag (net aerodynamic drag)	31	D	60·01	N
Lift-to-drag ratio (at the kite: real kite with mass)	39	LTD_k	4·77	
Resultant force, top of the line (real kite with mass)	40	T_k	292·7	N

https://doi.org/10.1017/S0001924000001469 Published online by Cambridge University Press

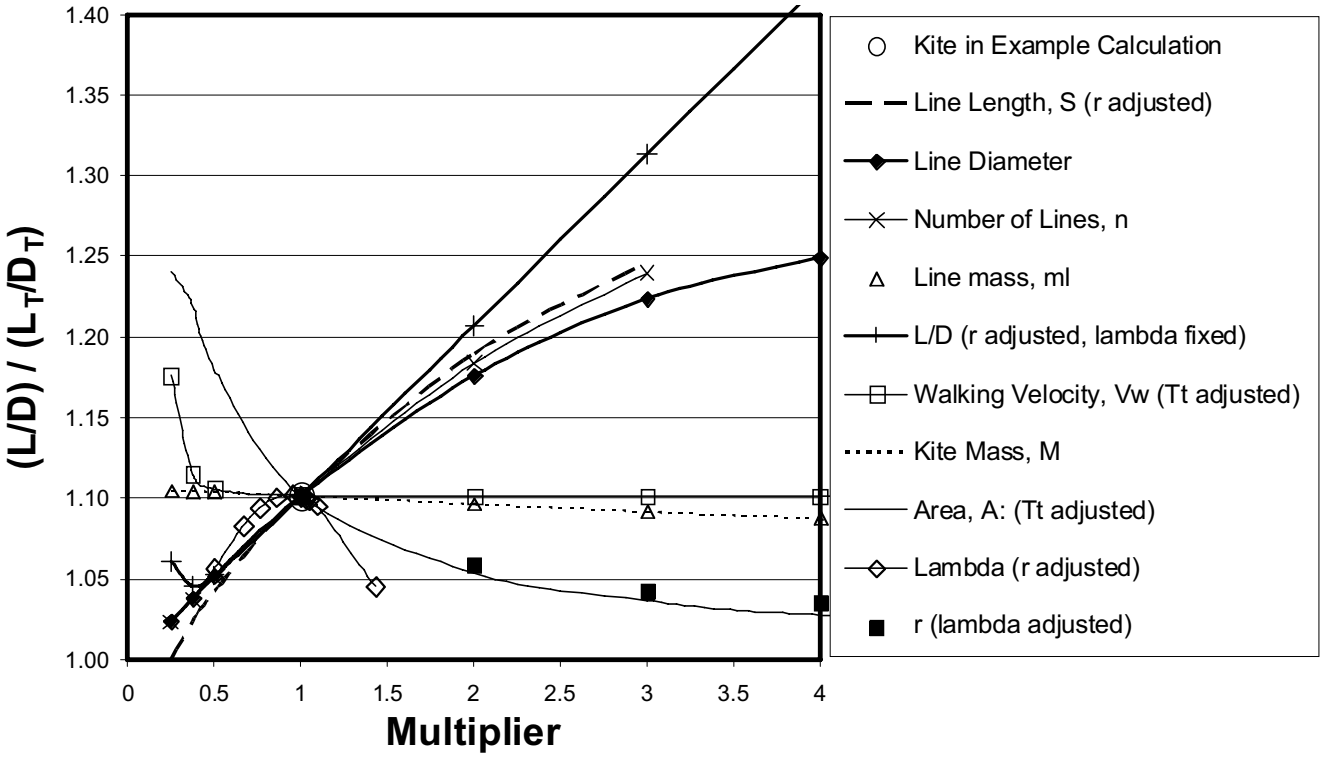


Figure 15. Sensitivity diagram: Ratio of aerodynamic L/D, to the circular testing L_T/D_T; for multiples of the shown variables, for the kite in the example calculation set.

While these results are only for one kite, in Fig. 13 it can be seen that:

1. The margins of error are significantly smaller for circular flight testing than were achievable from the car tests. (This was the main result in Ref. 2)
2. Both the raw results and the modified results from circular flight testing are within the experimental error of the car test results.
3. The modified circular flight test results are only a little different than the raw circular flight test results.
4. The experimental error (for circular flight testing) is smaller than the scale of the modifications. This means that making the modifications given in this paper will improve the accuracy of the results (at least for the tests in Fig. 13)

In Fig. 14 showing the lift coefficients, it can be seen that:

1. The margins of error for lift coefficients shown are about the same for the car rig and for circular flight testing. However, the large error in the circular test method results in this case was primarily due to poor measurement technique rather than limitations of the method itself. The testing method can be easily altered to improve the accuracy of the lift coefficient.
2. All three sets of results are closely grouped within experimental error of each other.

Tables 1 to 8 illustrate the correction process with a realistic sample set of measurements.

6.0 SENSITIVITY ANALYSIS

Building on the test setup of Tables 1 to 8, Fig. 15 (a necessarily numerical model) shows how much the net aerodynamic L/D, varies from the raw test L_T/D_T, for changes in various components in the test. The purpose of this is to give an indication as to when it will be more important to use the modifications of this paper.

For example the figure shows that the net L/D ratio for the test kite is 10% larger than the raw L_T/D_T directly from the tests. It also shows that if the kite area, A were to be doubled, then the $(L/D)/(L_T/D_T)$ would only be about 1·05 rather than 1.1, meaning that the actual L/D ratio is only 5% larger than the raw L_T/D_T. But if the line diameter were to be doubled, then the ratio would be about 1·18, and the raw results would be 18% less representative of the true L/D.

From this figure it is clear which variables have the largest effect on circular testing:

- Increasing or decreasing the number of lines and increasing the line diameter have a significant effect.
- The kite area has a significant effect if it is decreased (that is, if the kite is small relative to the size of the lines)
- If the L/D is large, this too has a significant effect.
- Changes in the kite mass, walking velocity and line mass have a minimal effect.

Adjusting the measured angle λ, by altering r was suggested in Ref. 2 as a way of reducing the error of measurement at high L/D. The effect of altering λ is shown to reduce the $(L/D)/(L_T/D_T)$ ratio from the example case.

https://doi.org/10.1017/S0001924000001469 Published online by Cambridge University Press

It should be noted that in the calculations for Fig. 15:

- It has been assumed that the kite characteristics remain constant. Only the variable in question was changed, unless it would in practice change another. In that case the secondary variable has been altered appropriately and noted in the legend. (For example if the walking speed has doubled, the line tension will increase by four times for the same kite.)
- The same kite L/D was maintained throughout except for the case of the change in L/D itself.
- Some of the plotted lines terminate because the results are incalculable with the given kite.

It is instructive to note that the tests of Figs 13 and 14 used 10m lines while the calculation set for Fig. 15 used 30m lines. Because of the smaller effect of the shorter 10m lines, the raw L_T/D_T results in Figs 13 and 14 should be closer to the actual L/D, than results those in the calculation set and Fig. 15. This can be seen to be the case, as in Fig. 13 the discrepancy seems about 4%, a better match than the 10% of Fig. 15. This supports the results shown in Fig.15.

7.0 CONCLUSION

The difference between the raw results of circular flight testing and the results of traditional kite tests was a potential disadvantage of this novel circular flight test method. But by using the modifying equations of this paper, the scale of the differences between the two methods has been shown to be small in most cases. And for those cases where the effects of circular testing are large, the modifying factors of this paper provide a method of correction.

From this paper it can be concluded that in many practical instances the raw results from circular flight testing will be all that is needed, while the scale of any discrepancies can be anticipated from the sensitivity analysis. On the other hand, once the modifying equations are encoded, the corrections are straightforward so that conventional results can be derived quickly from any measurements made.

Practical experience with full scale kites has shown that for rapid repeatable results, indoor tests are almost essential to get away from the vagaries of natural wind and weather. Circular flight type tests make these objectives achievable. Now that these tests have been devised, it remains for the practitioner to access a suitable building and set up the apparatus so that measurements can be taken at a rate that, for once, outpaces the kite making process.

REFERENCES

1. STEVENSON, J.C. Traction Kite Testing and Aerodynamics, 2003, PhD thesis, University of Canterbury.
2. STEVENSON. J.C., ALEXANDER, K.V. and LYNN, P. Kite performance testing by flying in a circle. *Aeronaut J*, 2005, **109**, (1096), pp 269-276.
3. ALEXANDER K.V. and STEVENSON J. A test rig for kite performance measurement, 2001, Proceedings of Institution of Mech Engineers, **215**, Part B, pp 595-598.
4. GEOLA, J.S., SOMU, N., ABEDINZADEH, R. and VIJAKUMAR, R. Wind loading effects on a caternary, *J Wind Engineering and Industrial Aerodynamics*, 1985, **21**, pp 235-249.
5. HOERNER, S.F. *Fluid Dynamic Drag*, 1965, USA.
6. ALEXANDER, K.V. and STEVENSON. J.C. Kite Equilibrium and bridle length, *Aeronaut J*, 2001, **105**, (1051), pp 535-541.

https://doi.org/10.1017/S0001924000001469 Published online by Cambridge University Press